

EXPERIMENTAL STUDY ON THE BEHAVIOR OF SFRC COLUMNS UNDER SEISMIC LOADS

F. GERMANO^{*}, G.A. PLIZZARI^{*} AND G. TIBERTI^{*}

^{*} University of Brescia, DICATA

Department of Civil, Architectural, Environmental and Land Planning Engineering,

Via Branze 43, 25123 Brescia, Italy,

e-mail:federica.germano@ing.unibs.it

e-mail:giovanni.plizzari@ing.unibs.it

e-mail:giuseppe.tiberti@ing.unibs.it

Key words: Steel Fiber Reinforced Concrete, columns, earthquake resistant structure, bi-axial load, ductility.

Abstract: The use of Steel Fiber Reinforced Concrete (SFRC) in columns was experimentally evaluated with the aim of reducing the stirrups spacing without compromising the columns seismic behavior in terms of drift capacity and dissipation energy.

Results from eight RC columns and eight SFRC ones are reported. The columns were reinforced with hooked steel fibers with a volume fraction of 1.0%, subjected to earthquake-induced displacement reversals and constant axial loads. The spacing and the diameter of the stirrups were varied in order to verify their influence, moreover mono-axial and bi-axial quasi-static tests were performed by keeping constant the vertical load.

The tests results confirmed that SFRC can reliably reduce the damage by preventing the concrete cover to spall out at earlier stages and increase the initial stiffness and the energy dissipation of the columns, especially for mono-axial loads that resulted a less severe load condition with respect to the bi-axial one. Nevertheless, it seems that, despite the fibers addition, the increased spacing reduces the columns ductility.

1 INTRODUCTION

The structures designed for seismic loads recommended by design codes can survive strong ground earthquake motions only if they have sufficient ability to dissipate seismic energy. This energy dissipation is provided mainly by inelastic deformations in critical regions of the structural system and requires adequate ductility of elements and their connections.

In the last decades, several researches have established that steel fibers produce significant improvements in engineering properties of concrete by providing toughness to the concrete matrix [1-3]. Steel Fiber Reinforced Concrete (SFRC), in fact, exhibits substan-

tially larger strain capacity as compared with traditional concrete, which makes its ideal for use in member subjected to large inelastic deformation demands such as beams, beam-column joints and columns-foundation joints.

Most of the researches was concentrated on the static loads and SFRC has been recognised a promising material for several structural applications such as floors, pavements [4] and tunnel segments [5]. Concerning the cyclic solicitations, SFRC improves the fatigue life [6] especially in the low-cycle region [7] and seems to be promising for seismic use in shear critical elements such as beam to column joints [8] or flexural critical element such as

columns-foundation joints [9-10].

The main objective of this paper is the evaluation of the cyclic behavior of SFRC for a possible use (in combination with traditional reinforcement) in columns of RC frames. In particular, it is investigated if fibers may be added to transverse reinforcement for increasing structural ductility and for reducing the stirrups concentration in joint regions. Special attention is devoted to highlight the role of steel fibers in changing the dissipated energy, the ductility and the damage configuration.

To this aim, an extensive experimental program was conveniently designed and the results will be presented herein. Experiments were performed on RC columns, with and without fibers; quasi-static horizontal reversal loads were applied by keeping constant the vertical load.

The influence of fiber addition, stirrups space and steel properties were investigated.

Since earthquake-induced lateral loading on building will not, in general, act along a principal axis of the structure (thus, columns with rectangular cross sections in such structures will generally be subjected to biaxial bending), the research program includes tests with load orientated in two different directions with respect to the principal axes of the section of the column (0 and 45 degree).

2 EXPERIMENTAL PROGRAM

Sixteen columns were tested at the University of Brescia for evaluating the contribution provided by fiber reinforcement under severe seismic loading conditions, both in terms of structural response (hysteretic behavior, strength stiffness and energy dissipation) and of damage level.

The full-scale column specimens, representing cantilever elements (from the foundation to the point of contraflexure), including eight SFRC columns and eight RC ones, were subjected to quasi-static reverse cyclic lateral loads, using either mono-axial and bi-axial horizontal loading (Fig. 1).

The specimens were designed according to the Italian Standards [11] by considering a corner column of a three storey seismic resis-

tant frame structure under a ground motion of 0.25 g. Four main parameters were investigated: dosage of fibers, type of steel and spacing of the transverse reinforcement and loading direction.

The complete experimental program is summarized in Table 1.

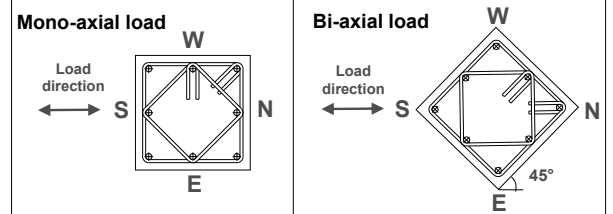


Figure 1: Mono and bi-axial horizontal load configurations.

Table 1: Experimental program

Spec	Horiz. load	Mate- rial	Transverse reinforcement		Axial Load		
	Mono/ Biaxial	[-]	Steel	n.	Spa- cing [mm]	N [kN]	N/ $f_c A_g$ [%]
P01	B		B450A				
P02	M			1+1			
P03	B	Plain	B450C		$\emptyset 8$		
P04	M	R _{ck}					
P05	M	45MPa	B450A			80	
P06	B			1+1			
P07	M		B450C		$\emptyset 6$		
P08	B						
P09	M		B450C			190	6.03
P10	B			1+1		80	
P11	M	SFRC			$\emptyset 8$		
P12	B	- 1%	B450C			100	
P13	M	R _{ck}					
P14	B	45MPa	B450C		1+1	80	
P15	M				$\emptyset 6$		
P16	B		B450C			100	

2.1 Materials and specimens geometry

All columns, cast horizontally, have a 300x300 mm cross section and a height of 2400 mm. In order to guarantee a rigid joint at the foundation, a footstall was properly designed. It consists of a steel footstall buried into the concrete; the space between the steel and the column was filled by a special concrete mixture with a mean compressive strength (after three days of curing) of about 50 MPa. The columns were inserted in the footstall for 600 mm; hence, the clear height was 1800 mm, while the distance between the point

load and the foundation was 1565 mm (Fig. 2). The base footstall simulates a rigid floor system or a rigid foundation while the load point application represents the middle of a double-curvature column; hence, only one half of the column was tested as a cantilever column, representing a double curvature column of about 3100 mm.

8D16 longitudinal rebars (B450C) were placed uniformly around the perimeter of the cross section, resulting in a longitudinal reinforcement ratio of 1.79%, and the nominal clear concrete cover was 35 mm.

Concerning the transverse reinforcement, D6 or D8 stirrups were spaced at 80 or 100 mm in the plastic hinge (Fig. 2); outside the critical region, the space was doubled except the top of the columns where extra ties were placed in order to prevent crushing of concrete due to the axial load applied. The amount of the transverse reinforcement was determined according to Italian Standards requirements for high (D8/80) or low (D6/80) ductility levels ("A" and "B" class). Two different types of steel were used (B450A and B450C) in order to investigate their influence.

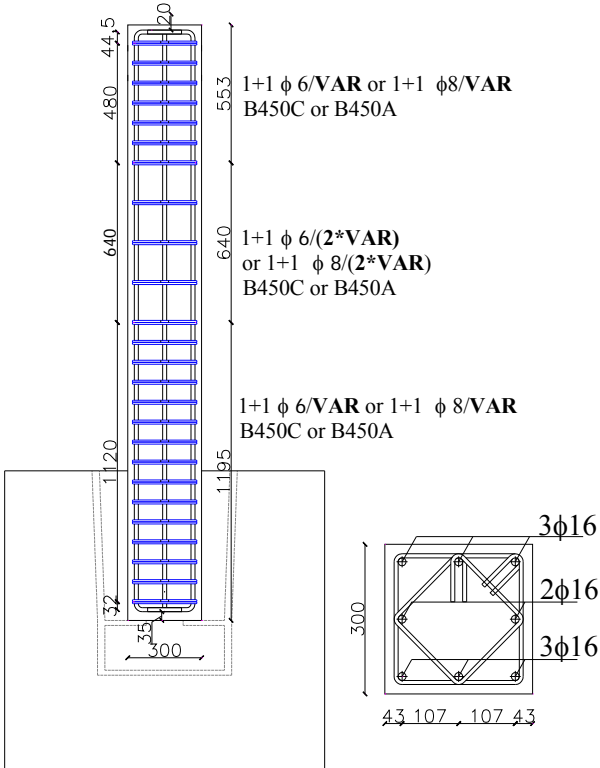


Figure 2: Geometry and reinforcement of the columns.

The designed strength class of concrete was C35/45. The aggregate had a maximum size of 16 mm. Slump class S5 and durability class XC3 were assumed. Two concrete batches were prepared: one reference batch with plain concrete (from P01 to P08), while the others had the same matrix with the addition of fibers (from P09 to P16).

Hooked fibers, 35 mm in length and 0.55 mm in diameter (Tab. 2), were added at the concrete plant with a dosage of 1.0% by volume (78.5 kg/m^3).

The compressive strength (R_{cm}), the Young Modulus (E_{cm}) and the tensile strength (f_{ctm}), obtained from the tests are reported in Table 3. The plain concrete batch has a strength ($R_{cm} \approx 50 \text{ MPa}$) very close to the specific target strength, whereas SFRC has a concrete class lower than the design value ($R_{cm} \approx 42 \text{ MPa}$). This was probably due to the higher porosity of SFRC, as it was confirmed by the lower density of SFRC specimens. For the same reasons, fiber addition seems to diminish the elastic modulus; further details are reported elsewhere [12].

The average values of the mechanical properties of the rebars adopted are reported in Table 4. As one can observe, the steel B450A showed the lowest values of A_{gt} which is the total deformation at the maximum load or rather a measure of the material ductility.

Table 2: Geometrical and mechanical properties of the fibers.

Material	Diameter d_f [mm]	Length L_f [mm]	Aspect ratio L_f/d_f	Tensile strength f_{ft} [MPa]
Low carbon	0.55	35	65	1100

Table 3: Average values for the main mechanical properties of the concrete matrix.

Material Type	Spec. weight [kg/m ³]	R_{cm} [MPa]	E_{cm} [MPa]	f_{ctm} [MPa]
NSC	2308	50.46	34204	2.83
NSC-SFR	2279	42.17	33556	2.76

The fracture properties of SFRC were determined according to the European Standard

[13] which requires bending test (3PBT) on notched beams (150x150x550mm). The tests were carried out with a closed-loop hydraulic testing machine by using the Crack Mouth Opening Displacement (CMOD) as control parameter that was measured by means of a clip gauge positioned astride a notch (having a depth of 25 mm) at midspan. Linear Variable Differential Transformers (LVDTs) were used to measure the Crack Tip Opening Displacement (CTOD) as well as the vertical displacement at mid-span under the load point. The fracture parameters and the classification according to the international requirements [14] are reported in Table 5.

Table 4: Average values for the main mechanical properties of the rebars.

Reinforcement	Young modulus	Yielding	Rupture	A_{gt}
	[GPa]	[MPa]	[MPa]	[%]
rebars $\Phi 16/C$	195.0	547.0	651.8	12.5
stirrups $\Phi 6/C$	196.7	530.2	603.4	10.9
stirrups $\Phi 6/A$	215.6	552.2	592.4	4.5
stirrups $\Phi 8/C$	198.6	501.2	635.4	11.9
stirrups $\Phi 8/A$	190.7	542.4	569.8	4.8

Table 5: Fracture properties of SFRC.

3PBTs results	UNI EN 14651				
	f_L [MPa]	f_{R1} [MPa]	f_{R2} [MPa]	f_{R3} [MPa]	f_{R4} [MPa]
Mean Value	7.03	6.86	6.7	6.07	5.44
Standard Dev.	1.01	1.01	1.06	0.98	0.92
Charact. value	5.07	5.03	4.77	4.3	3.77
MC2010 class			5b		

2.2 Testing procedures

In order to simulate the loads and keep the boundary conditions of the specimens as close as possible to the real case, a computer-controlled testing system with a displacement control was used with a steel reacting frame (Fig. 3). The latter was fixed to the strong floor by using dywidag bars conveniently post-tensioned in order to prevent the rotation; the same was done for the footing pad with four dywidag bars. With the aim of avoiding any translation of the steel frame and the foundation, a shear reacting frame was designed: a girder was connected both to the steel frame and to the foundation pad by means of post-

tensioned dywidag bars.

A mono-axial and a bi-axial lateral load configurations (with an angle of 45deg) were used (Fig. 1). To apply the lateral load, an electromechanical screw jack, with a maximum thrust capacity of 200 kN and a ball screw spindle was used and the steel devices employed are represented in Figure 4a,b for the mono and bi-axial loading respectively. The vertical load was applied by post-tensioning an internal unbonded strand with a hydraulic jack.



Figure 3: Steel reacting frame and test set-up.

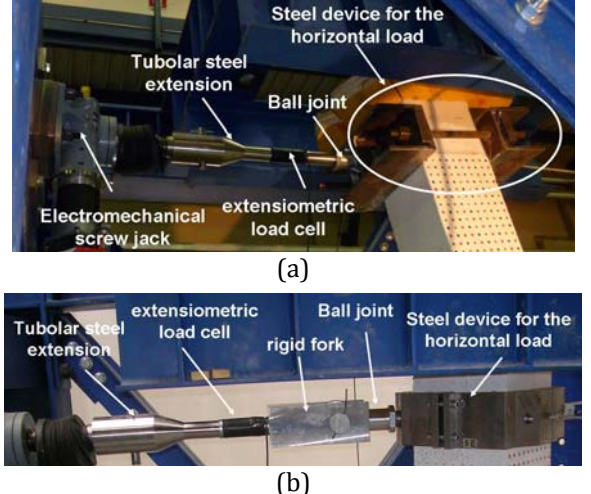


Figure 4: Steel device for the screw jack-column connection for mono (a) and bi-axial (b) load configurations.

The loading conditions (lateral displacement and axial load histories) were chosen equal for all the columns. The axial compressive load was equal to $0.06 f_c A_g$ and it was

kept constant during the test. The lateral load was applied through a quasi-static protocol; the tests were performed under displacement control and the rate of lateral loading varied between 0.4 mm/min for the low displacement cycles to 9 mm/min for the large ones.

The sequence of reversing lateral load (Fig. 5) was developed according to the ACI T1.1-01 requirements [15]. The displacement history during the test was characterized by:

- initial drift ratios within the essentially linear elastic response range for the column;
- displacements applied by gradually increasing drift ratio until 6.5%;
- three fully reversed cycles applied at each drift ratio.
- monotonic displacement increase beyond the 6.5% drift ratio or up to the failure of one of the longitudinal bars.

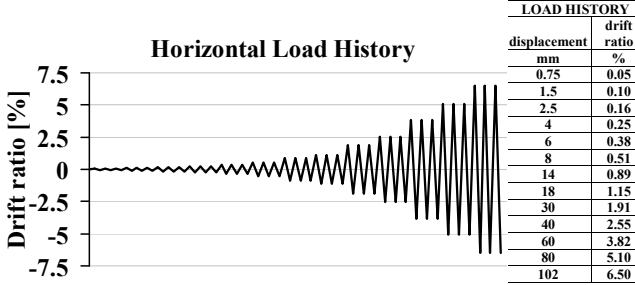


Figure 5: Horizontal load history.

The horizontal and the lateral loads were monitored by means of two load cells; the horizontal displacement was recorded by using linear displacement potentiometers settled according the scheme reported in Fig. 6a. As shown in Figure 6b, linear displacement potentiometers (with metal rod-end bearings at both ends of the sensor) were installed on the column to measure the vertical displacements at various levels over the height of the column, in order to find the column curvature. Finally, two LVDTs were settled in order to monitor the steel frame and foundation displacements, together with three other LVDTs used to measure the rotation and the displacement of the filling mortar.

Moreover, the rebars and the stirrups in the plastic hinge region were also equipped with a series of strain gauges (Fig. 7) in order to better understand the real behavior of the steel reinforcement. Further details about set-up

layout and instrumentation of the specimens are presented elsewhere [12].

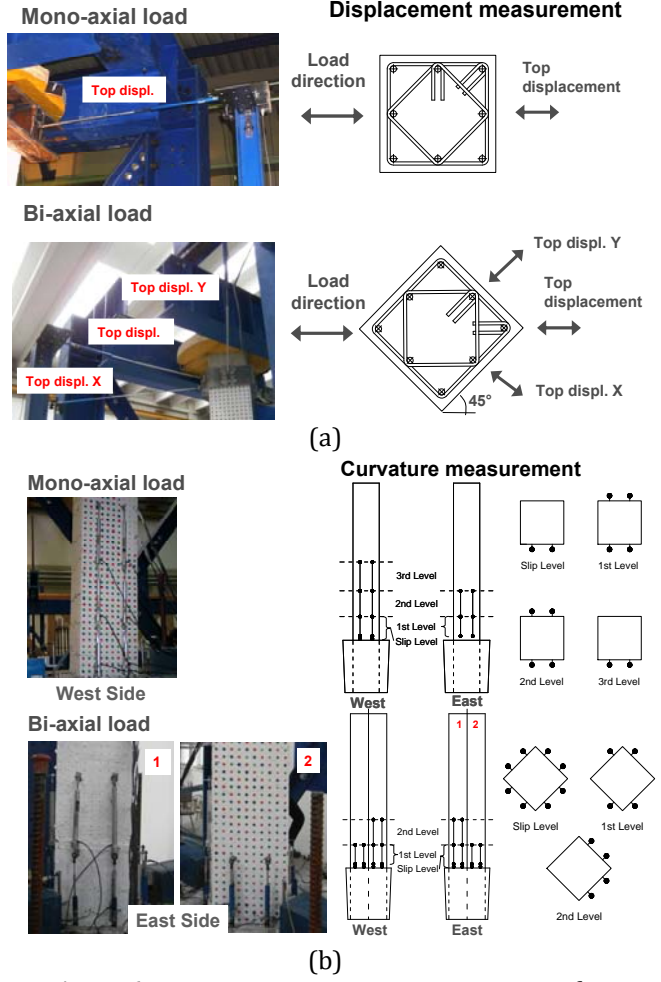


Figure 6: Linear potentiometers arrangement for displacement (a) and curvature (b) measuring in both the horizontal load configurations employed.

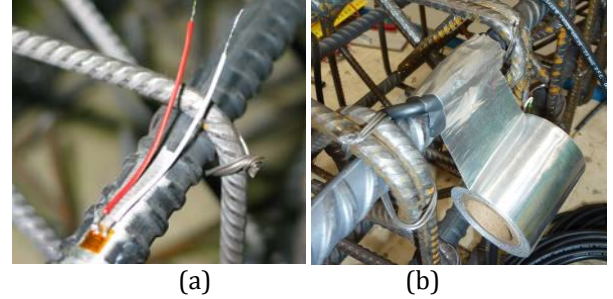


Figure 7: Strain gauges wiring (a) and coating (b).

3 RESULTS DISCUSSION

This section provides a summary of the test results by including damage observations and presenting the engineering quantities such as load, moment, average curvature, ductility and energy dissipation. Further details of each issue are reported elsewhere [16].

3.1 Damage distribution and crack pattern

A qualitative description of damage progression and the corresponding damage states at different drift ratio can be drawn with the help of important damage parameters that can be recognized as location, width, and orientation of the cracks, yielding of longitudinal reinforcing bars, spalling of concrete cover, buckling of longitudinal bars together with opening of tie hooks, and crushing of concrete core. Most of the just abovementioned aspects are related to different damage states that in the literature are classified in several ways according to the available standards [11 and 17].

By way of example, the comparison between two mono-axial specimens (RC and SFRC) and two bi-axial ones is reported in Figure 8 and Figure 9 respectively, whereas the numerical values for maximum crack width, crack spacing and crushing region for all the specimens are compared from Figure 10 to Figure 12.

For all the specimens, the major damage was observed just above the footing and the collapse took place, when a longitudinal bar broke after the development of a severe buckling. The SFRC specimens tend to localize the damage at the base foundation more than the RC ones (Fig. 8d and Fig. 9d).

It was observed that the first crack appears at 0.25% of drift ratio for the mono-axial specimens and one drift level before for the bi-axial ones. For both the horizontal load direction applied and the RC and SFRC specimens, the cracked region continuously increased up to a drift level of 1.91%, stabilizing around 1100 mm, whereas the crack spacing decreased reaching a value which is generally lower with fibers for both the mono and bi-axial tests (Fig. 10). Moreover, the SFRC columns showed lower crack width with respect to the plain concrete ones, although this tendency seems more remarkable after the 1.15% of drift ratio (Fig. 11). As far as the crushing is concerned, it can be definitely stated that fibers limited the spalling off of the concrete cover.

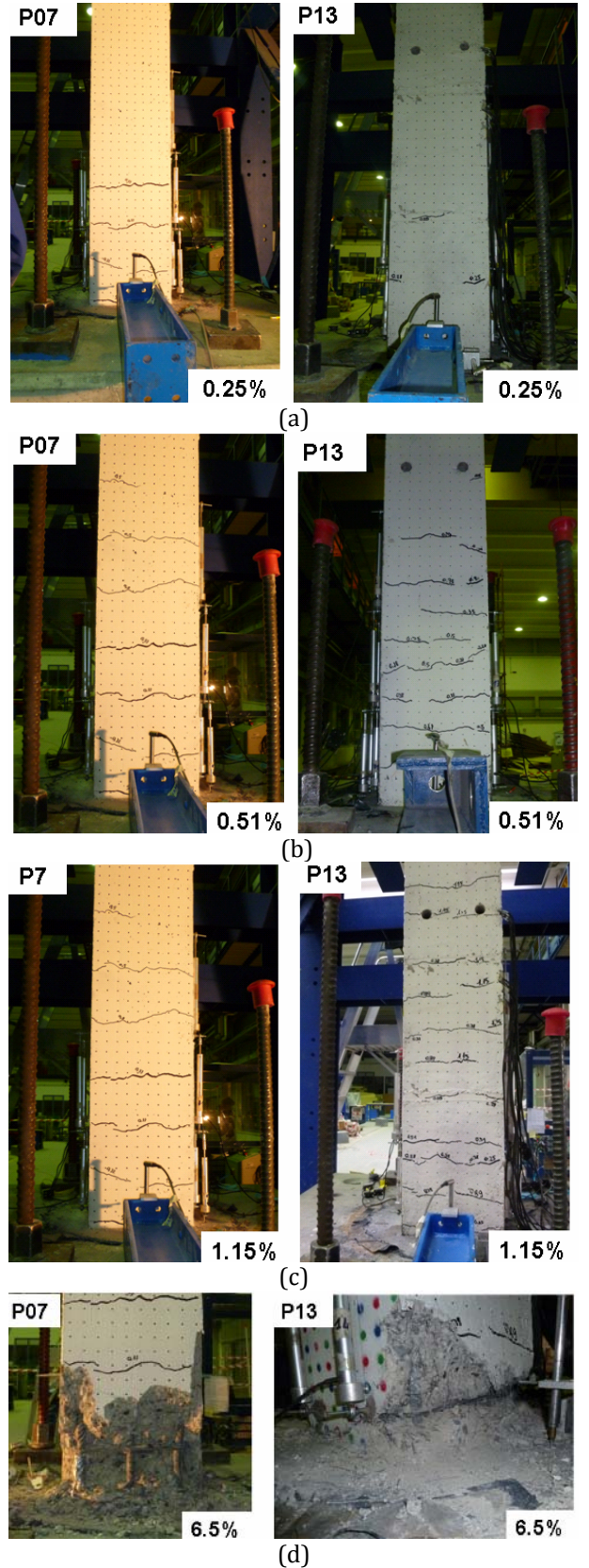


Figure 8: Damage distribution along the column at different drift levels for two specimens (with and without fibers) mono-axially tested: (a) first cracking stage; (b) 0.51% (damage state); 1.15% (yielding limit); (d) 6.5% or more (end of the tests).

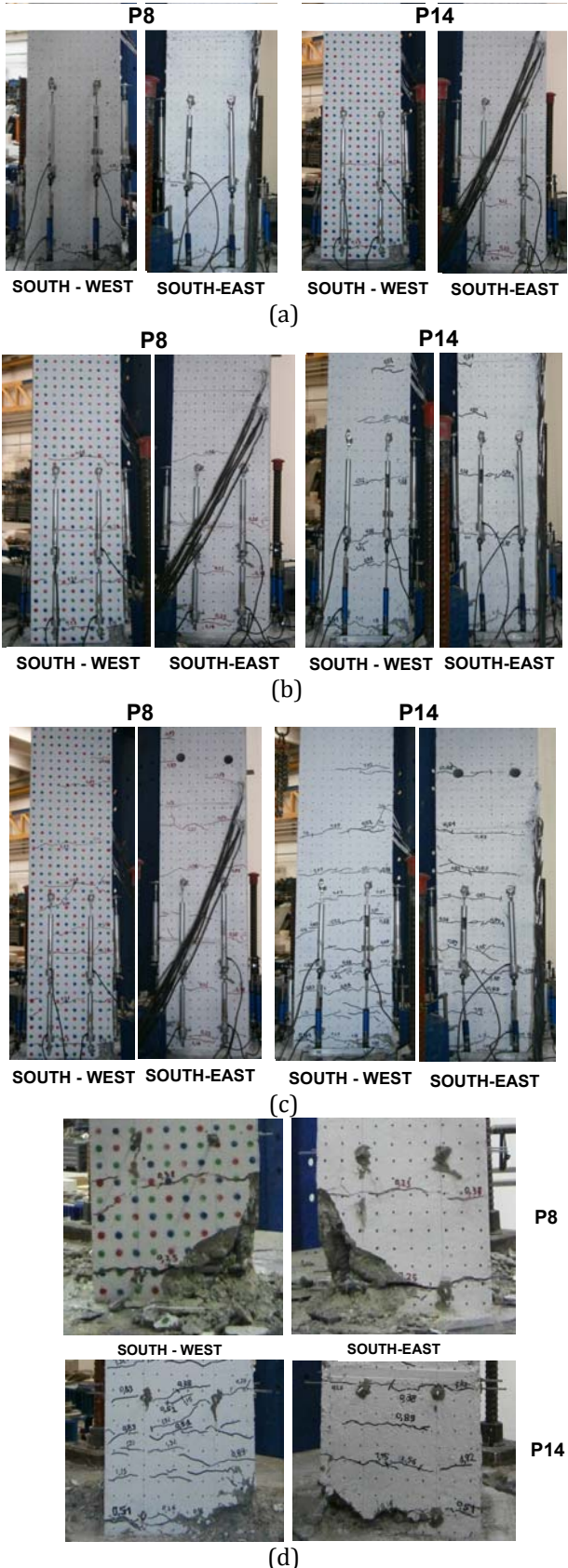


Figure 9: Damage distribution along the column height at different drift levels for two specimens (with and without steel fibers) bi-axially tested: (a) first cracking stage; (b) 0.51% (damage state); 1.15% (yielding limit); (d) 6.5% or more (end of the tests).

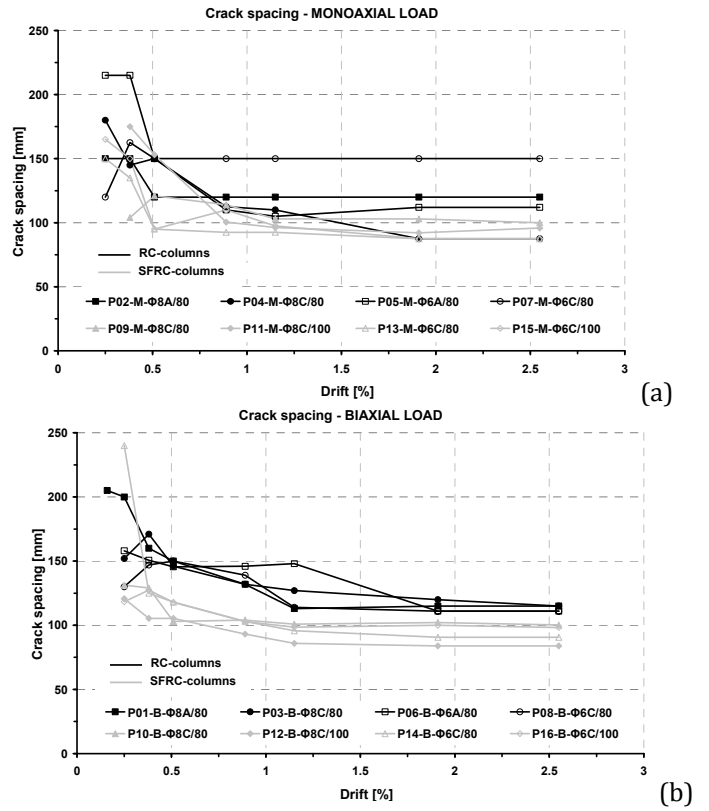


Figure 10: Crack spacing for the mono-axial specimens (a) and the bi-axial ones (b).

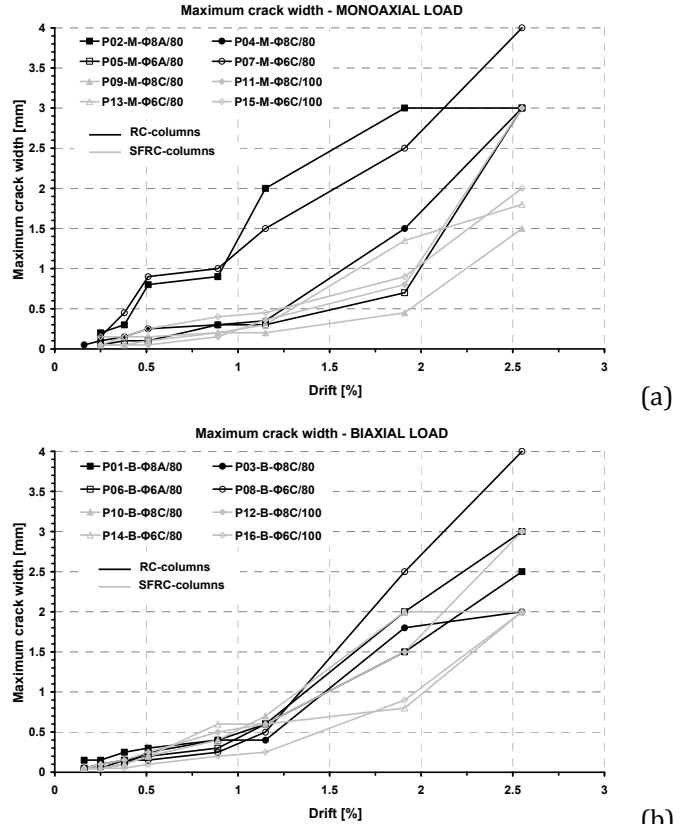
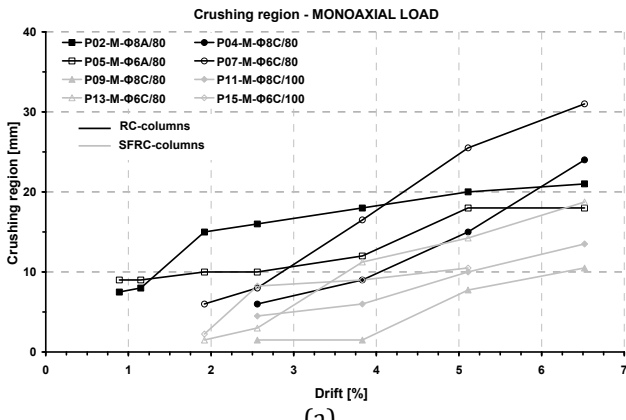


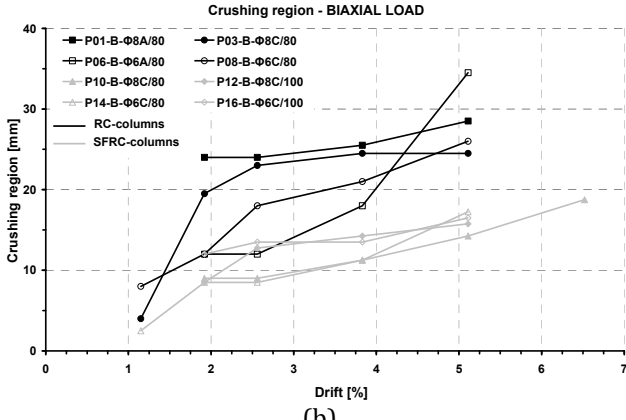
Figure 11: Maximum crack width for the mono-axial specimens (a) and the bi-axial ones (b).

Generally, the crushing of the SFRC col-

umns started one or two drift after with respect to the RC ones; the crushed zone remained always lower in the SFRC columns and the trend was more pronounced when a bi-axial load was applied (Fig. 12). While the plain concrete specimens exhibited a severe concrete spalling off and buckling of the longitudinal rebars, the SFRC concrete cover was cracked and damaged but did not spalled out completely, due to the fiber action. No signs of noticeable buckling were noticed for the longitudinal bars of the SFRC specimens which were not completely exposed even at the end of the tests.



(a)



(b)

Figure 12: Crushing for the mono-axial specimens (a) and the bi-axial ones (b).

3.2 Horizontal load vs. displacement

In Figure 13, the comparison between load vs. top displacement curves for two specimens, that differ only for the addition of fibers, is depicted. The displacement plotted comes from the linear displacement potentiometer, since the steel reacting frame, the foundation pad and the cementitious filling displacements were negligible. For both the specimens, a

typical flexural behavior appears, with no pinching effect.

The addition of fibers seems to moderately increase the initial stiffness of the columns and in case of bi-axial loading also the strength, although a clear tendency can not be observed. The ultimate displacement of the RC columns generally is higher than that of the SFRC ones (Fig. 14). However, due to the increased stiffness, the global ductility of the SFRC columns (especially for those tested under mono-axial load) increased. Anyway, when an higher stirrups spacing is employed the ductility decreased seriously (P09 vs. P11 and P13 vs.P15 in Fig. 15).

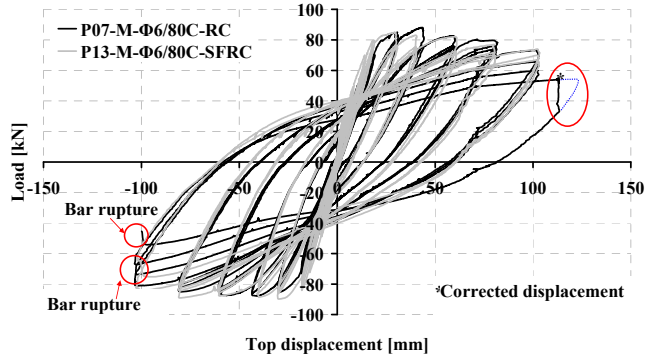


Figure 13: Typical load vs. top displacement curves: P07 and P13 comparison.

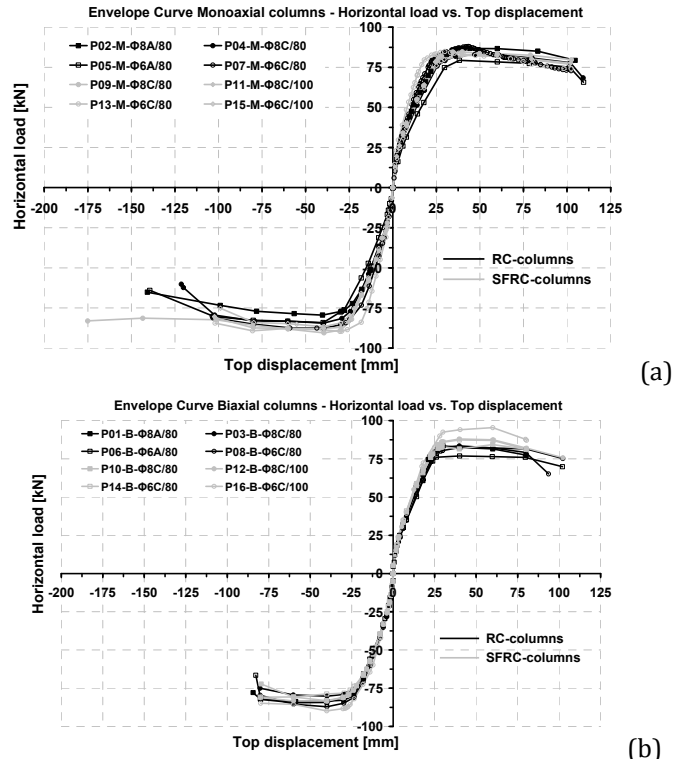


Figure 14: Envelope curves of all the specimens subjected to mono-axial load (a) and bi-axial one (b).

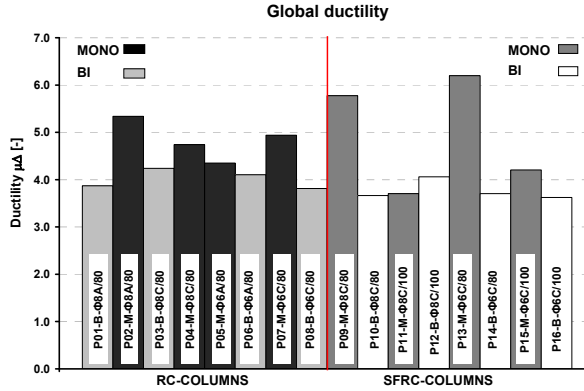


Figure 15: Global ductility for all specimens tested.

By applying a bi-axial load, the ultimate displacement generally decreased (Fig. 14a,b); thus the global ductility decreased and the tendency is more remarkable for the SFRC columns (Fig. 15).

The diameter of the transverse reinforcement, as well as the type of steel (B450A), does not seem to have had remarkable effects with reference to the global behavior of the columns.

3.3 Moment vs. curvature

By plotting the moment vs. curvature curves, the local behavior is investigated and the same tendencies observed in term of global behavior (load vs. displacement curve) seem to turn out. In this case the envelope curves for the RC specimens and the SFRC ones are depicted in Figure 16a,b respectively.

When a bi-axial load is applied, the ultimate curvature diminishes (with or without the fibers addition), whereas the initial stiffness of the RC columns seems to increase.

By applying a mono-axial load, the local ductility of the SFRC specimens is generally higher than that of the RC ones (also when a larger stirrup spacing is employed), while the opposite tendency is noticed for the bi-axial load condition (Fig. 17).

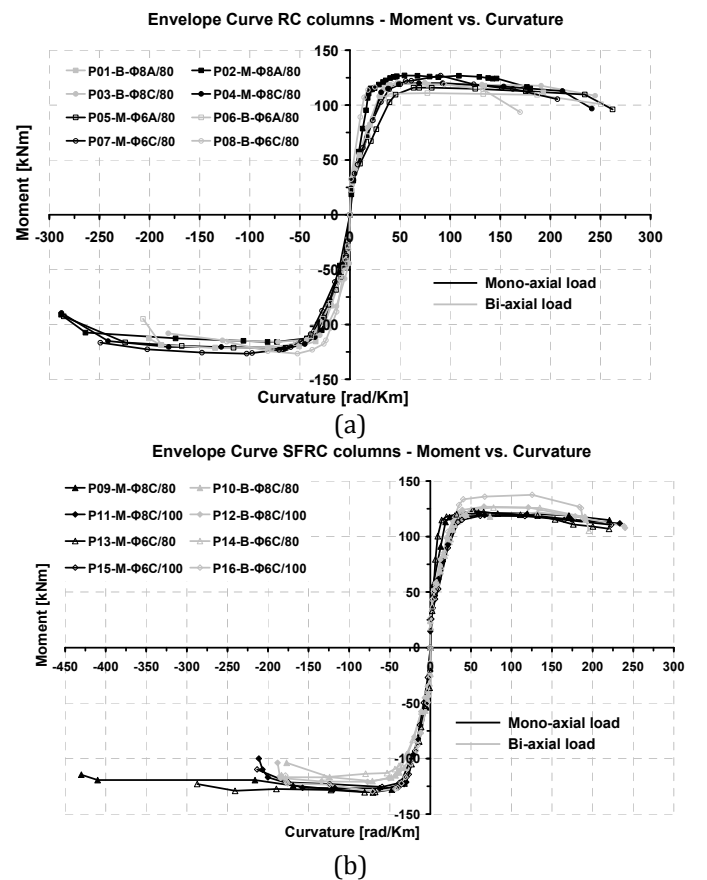


Figure 16: Envelope curves of all the RC columns (a) and the SFRC ones (b).

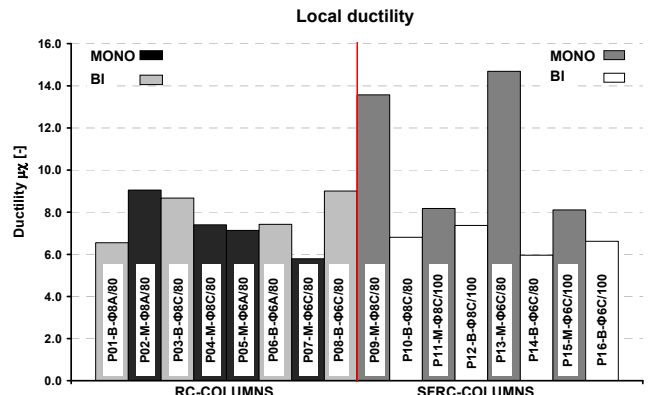


Figure 17: Local ductility.

3.4 Energy dissipation

With the aim of quantifying the columns response, it is desirable to define efficiency indexes that quantitatively describe the columns behavior. In seismic design, the inelastic deformation is generally quantified by ductility parameters, presented in the previous paragraph and by energy dissipation capacity, which is of paramount importance for the evaluation of the seismic performance of a

structural member. In fact, when earthquakes occur, energy is injected into the structure and has to be dissipated by the structure itself; when the structure is no longer able to dissipate energy, the collapse occurs. The measurement of the dissipated energy could thus become a good efficiency index.

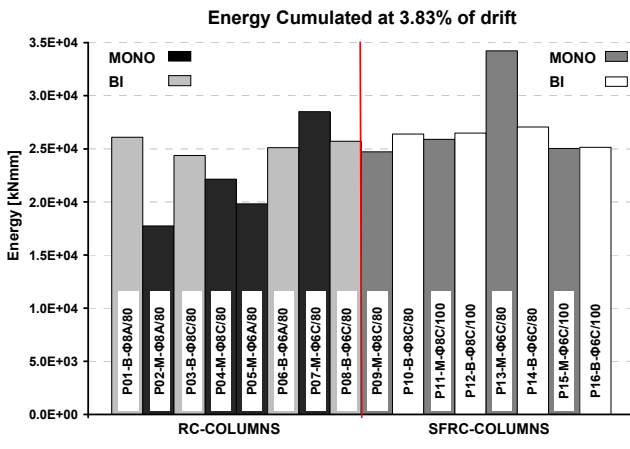


Figure 18: Cumulated energy.

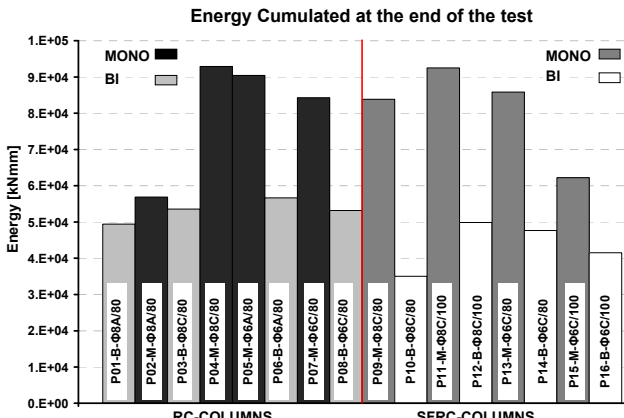


Figure 19: Cumulated energy at the end of tests.

For a fixed value of 3.83% drift ratio, when a mono-axial load is applied, it can be observed that the SFRC columns dissipate more energy than that of the RC ones; this tendency is less pronounced in case of the bi-axial load condition. Moreover, in RC specimens, it has been generally observed that the cumulated energy of the columns bi-axially loaded is generally higher than that of those mono-axially loaded.

When considering the end of the tests, it can be observed that the dissipated energy drastically diminishes when a bi-axial load is applied due to the lower number of cycles at

failure of the specimens. In case of mono-axial load, the SFRC specimens guarantee an energy dissipation a little bit higher than that of the RC ones (except for the specimen with a stirrup spacing of 100 mm and diameter of 6 mm); when the biaxial load condition is considered, the addition of fibers seems to be less effective and the RC columns dissipate more energy than that of SFRC ones.

4 CONCLUSIONS

The flexural behavior of reinforced concrete columns, with and without the steel fibers addition, subjected to bending tests about a section diagonal and about a principal axis, was investigated through an extensive experimental campaign. The influence of different types of stirrups steel and of the amount of transverse reinforcement was studied.

The comparison of the test results highlighted that there was little difference between the flexural strength for bending about a section diagonal (bi-axial load) and for a bending about a principal axis (mono-axial load). However, the bi-axial load turned out as a more severe load condition, reducing both the available ductility and the energy dissipation.

The influence of the fiber addition seemed to be more pronounced in the mono-axial condition by increasing the dissipation energy and the ductility; nevertheless, when an higher stirrups spacing was employed, the ductility decreased seriously.

The addition of fibers enabled to reduce the damage by preventing the concrete cover to spall out at earlier stages and by reducing the buckling of the longitudinal bars which were not completely exposed even at the end of the tests.

ACKNOWLEDGEMENTS

The Authors would also like to give their strong appreciation to Sismic association for funding the research.

The Authors are thankful to eng C. Baldassari and eng D. Pezzotta for the constant assistance during the performing of the experimental tests. Sincere thanks are extended to the student M. Franceschini, V. Longo, L. Vacca

and to the technicians A. Botturi, D. Caravaggi, A. Delbarba for their support in the experimental research activities.

A special acknowledgement goes to Bekert Corp. for providing the fiber reinforcement.

REFERENCES

- [1] Di Prisco, M., Felicetti, R. & Plizzari, G.A. (Eds) 2004. *Proceedings of the 6th RILEM Symposium on Fiber Reinforced Concretes (FRC)*, Varenna (Italy), September 20-22, RILEM PRO 39, Bagneaux (France): 1514 pp.
- [2] Gettu, R. 2008, *Proceedings of the Seventh Intnl. RILEM Symp. on Fibre Reinforced Concrete: Design and Applications*, BEFIB-2008, 17-19 September, pp. 1154.
- [3] Barros, J.A.O. et al, *Proceedings of the Eighth RILEM Intnl. Symp. on Fibre Reinforced Concrete: challenges and opportunities*, (BEFIB 2012), 19-21 September, Guimarães.
- [4] Cominoli L., Plizzari G.A. 2006. SFRC precast slabs, *Proceedings of The Second Fib Congress*, Naples, Italy, 5-8 June 2006, abstract on page 460-461, full length paper available on accompanied CD.
- [5] Tiberti, G., Plizzari, G.A., C.B.M. Blom, Walraven J., 2008. Concrete tunnel segments with combined traditional and fiber reinforcement, in *Intl fib Symposium, Tailor Made Concrete Structures*, Amsterdam (the Netherlands), pp. 199-205.
- [6] Plizzari, G.A., Cangiano, S. and Cere, N., 2000. Post-peak Behavior of Fiber-Reinforced Concrete under Cyclic Tensile Loads, *ACI Mat. J.*, **97 (2)**: 182-92.
- [7] Germano, F., Plizzari, G.A., 2012. Fatigue Behavior of SFRC under Bending, in *Proceedings of the Eighth RILEM Intnl. Symp. on Fibre Reinforced Concrete: challenges and opportunities*, (BEFIB 2012), 19-21 September, Guimarães, Abstract on page 113-414, Paper on CD
- [8] Lee H.H., 2007. Shear strength and behavior of steel fiber reinforced concrete columns under seismic loading, *Eng. Struct.* **29**: 1253–1262
- [9] Palmieri, M., Plizzari, G.A., Pampanin, S. Mackechnie, J. 2008, Experimental investigation on the seismic behaviour of SFRC columns under biaxial bending, in *IC-CRRR 2008, Proceedings of the International Conference on Concrete Repair, Rehabilitation and Retro-fitting II*, 24-26 November, Cape Town (South Africa), Abstract on page 413-414, Paper on CD, ISBN: 978-0-415-46850-3.
- [10] Germano F., Plizzari G, Colombo A., Failla C., 2009. Experimental investigation on the behavior of Fiber Reinforced Concrete Precast Columns under cyclic load, *XIII Convegno nazionale “L'ingegneria sismica in Italia” ANIDIS 2009*, Bologna, ISBN 978-88-904292-0-0.
- [11] NTC 2008, *Norme tecniche delle costruzioni*, D.M. 14/01/2008, pp. 428.
- [12] Germano F., 2011. *Cyclic behavior of SFRC: from material to seismic columns*, Ph.D. Thesis, University of Brescia, pp. 433, in press.
- [13] UNI EN 14651, 2005. *Test method for metallic fiber concrete - Measuring the flexural tensile strength (limit of proportionally (LOP), residual)*, European Committee for Standardization, 18pp.
- [14] Model Code 2010, Final Draft, fib bulletins 65 and 66, International Federation for Structural Concrete (fib), April 2012.
- [15] ACI Innovation Task Group 1 and Collaborators, 2001. *Acceptance Criteria for Moment Frames Based on Structural Testing (ACI TI.1-01) and Commentary (ACI TI.1R-01)*, American Concrete Institute: 10 pp.

- [16] Germano F., Plizzari G.A., Baldassari C., Pezzotta D., Franceschini M., Vacca L., Longo V.. 2013. Behavior of SFRC Columns Under Seismic Loads, *Technical Report DICATA*, University of Brescia, in press.
- [17] FEMA Publication 273, 1997. Guidelines for the seismic rehabilitation of buildings.